

Role of oxygen admixture in stabilizing TiO_x nanoparticle deposition from a gas aggregation source

Amir Mohammad Ahadi · Vladimir Zaporojtchenko · Tilo Peter · Oleksandr Polonskyi · Thomas Strunskus · Franz Faupel

Received: 16 April 2013 / Accepted: 11 November 2013 / Published online: 30 November 2013
© Springer Science+Business Media Dordrecht 2013

Abstract For the use of a gas aggregation cluster source a high and stable deposition rate is desired. For many metals, nanoparticle formation is enhanced by admixture of reactive gases. Here, the role of reactive gas admixtures on the nanoparticle deposition rates is investigated for the case of reactive direct current magnetron sputtering of Ti in a gas aggregation chamber. The results show that, at low working gas (argon) pressures, stable cluster deposition at high rates can only be achieved for admixtures with a very narrow oxygen flow range. At higher pressures, stable deposition can be observed only after an intermediate maximum rate has been crossed or a stable deposition rate is not reached at all. For the different sputtering conditions, the partial pressure of oxygen was monitored with a mass spectrometer. The results are

explained in terms of the competing roles of oxygen in cluster nucleation as well as in target poisoning. The cluster size distributions for different conditions were characterized by scanning electron microscopy.

Keywords Stabilization · Nanocluster · Reactive sputtering · Aerosol nucleation · Cluster deposition

Introduction

Since many years, nanocluster research has evolved as a new and interesting field in nanoscience (Bauer et al. 1999; Kortshagen 2009; Schultes et al. 2007; Wilcoxon and Abrams 2006) particularly due to the exclusive features of clusters and their role in the transition from atomic scale to bulk material. Metal clusters—as one of most investigated class of clusters—show interesting physical (Anders et al. 2011; Baletto and Ferrando 2005; de Heer 1993) and chemical (Grabowska et al. 2010; Wilcoxon and Abrams 2006) properties. They also play an important role in the fabrication of new nanocomposite materials and in adjusting the properties of these materials (Biederman 2011; Faupel et al. 2010). The formation processes and applications of this type of clusters (Smirnov 2003; Wegner et al. 2006) are, therefore, an attractive field of research for many researchers from different disciplines.

Vladimir Zaporojtchenko: Deceased on 31.08.2012.

A. M. Ahadi · V. Zaporojtchenko · T. Peter · O. Polonskyi (✉) · T. Strunskus · F. Faupel (✉)
Faculty of Engineering, Institute for Material Science –
Chair for Multicomponent Materials, Kiel University,
Kaiserstr 2, 24143 Kiel, Germany
e-mail: polonskyi.oleksandr@gmail.com

F. Faupel
e-mail: ff@tf.uni-kiel.de

O. Polonskyi
Faculty of Mathematics and Physics, Charles University
in Prague, V Holesovickach 2, 180 00 Prague 8,
Czech Republic

Magnetron sputtering combined with a gas aggregation chamber, introduced by Haberland et al. (1992), is an attractive method for metal cluster production. For this method, several theoretical (Kashtanov et al. 2007; Smirnov 2000) and experimental (Hihara and Sumiyama 1998; Palmer et al. 2003; Shyjumon et al. 2006) studies were concerned with the effect of sputtering parameters and environmental conditions on cluster formation.

For some chemical elements, especially for highly reactive metal atoms which have low dimer binding energy, conventional direct current (DC) magnetron sputtering in combination with pure argon aggregation gas is not able to create stable cluster nuclei. Adding a small amount of reactive gas to the working gas is a typical solution for these elements. This method increases the probability of nucleation (and cluster growth) in collisions by production of compound molecules (Peter et al. 2012).

Many investigations (Drabik et al. 2011a, b; Faupel et al. 2010) considered cluster formation from reactive magnetron sputtering in the gas aggregation cluster source, but most of them focused on the properties of the deposited films (nanocomposite thin films as well as pure cluster films) and their applications.

Drabik et al. (2011a, b) studied the morphology and structure of Ti clusters films prepared by the Haberland method. The aging effect of samples produced at different magnetron currents and different pressures was also considered. They found (Drabik et al. 2011a, b) that when as prepared titanium cluster films are exposed to the air atmosphere, the deposited clusters oxidize immediately (and prepared films turn to transparent). However, they did not study the role of impurities (reactive gas) on cluster formation.

Recently, few studies tried to explain the role of reactive gas in cluster formation and seeding processes. Marek et al. (2011) investigated the effect of changing oxygen admixture (as a reactive gas) on cluster production at constant argon aggregation pressure and found that adding a small amount of oxygen can improve cluster generation dramatically. In a previous study (Peter et al. 2012) we analyzed the influence of the reactive gas on the formation process of transition metal clusters in a gas aggregation chamber. It was found that at each operation condition, cluster generation can only take place within a specific concentration range of reactive gas. Outside this range, no cluster formation takes place, since a

reactive gas flow below the minimum of the range cannot promote cluster nucleation, and a reactive gas flow higher than the maximum of the range leads to target poisoning, which decreases sputtering and thus makes cluster production impossible.

Stable cluster production at different conditions is important for technical applications. However, due to high reactivity of Ti and other reactive metal atoms, the stabilization of cluster deposition is very difficult. Furthermore, several complex processes, such as resputtering and oxide molecules formation in the volume and on the surfaces, influence the clustering processes in reactive sputtering and make stabilization of deposition quite complicated. To date, the influence of reactive gases on the stabilization of cluster production in a gas aggregation chamber has not studied for Ti or other metals, although, understanding of the underlying mechanisms is crucial to control the physical and chemical processes in the aggregation chamber during cluster formation, and hence the properties of deposited cluster films.

When reactive gas is added to the aggregation chamber, several processes can occur. The reactive gas can promote cluster nucleation by binding to the sputtered metal atoms and creation of compounds. These molecules have a much higher binding energy in comparison with binding between pure metal atoms and can accelerate the cluster nucleation process (and also cluster growth) in collisions (Peter et al. 2012).

The reactive gas can also cause poisoning of the target surface (Safi 2000). This takes place in two ways: The first one is diffusion or flow of reactive gas into the aggregation chamber. Thus, reactive gas molecules can arrive on the target directly and react with surface atoms and produce dielectric compounds on it. The second poisoning mechanism is that some oxidized metal atoms arrive on the target from the gas phase and are incorporated into the growing oxide. Other possible scenarios for oxygen molecules are sticking to the chamber walls and escaping from aggregation chamber via the orifice.

It is well-known (Depla and Mahieu 2008) that the number of sputtered atoms decreases strongly upon increasing fraction of poisoned active target surface. The number of sputtered atoms in turn and its affecting parameters (such as erosion area, power, and pressure) control the amount of reactive gas consumed in the different processes. In other words, the number of accessible sputtered atoms in the aggregation chamber

determines the quantity of reactive species consumed for compounds generation. Hence, by varying the working pressure not only the number of sputtered atoms, but also the number of molecules returning to the target can be changed. This means that just by adjusting the working pressure, the consumption rate of reactive atoms as well as the rate of surface poisoning can be tuned. Thus, we expect the deposition rate (D.R.) evolution and also the clustering processes to vary markedly with pressure.

According to the theoretical models (Kashtanov et al. 2007; Smirnov 2003), cluster production (and growth) take place in three steps:

1. Cluster nucleation via three body collisions.
2. Cluster growth by binding of single atoms.
3. Clusters coalescence.

During each reaction, some thermal energy is released and dissipated by the working gas particles. If they cannot transfer the released reaction energy completely, the remaining thermal energy can dissociate particles from the cluster. The final clusters size depends on the particle densities of the different species which contribute in the nucleation and growth processes, the cluster residence time in the aggregation chamber, and the temperature. The residence time is affected by the length of aggregation chamber, the working pressure, and the gas flow (Polonskyi et al. 2012).

In the present work, we considered the various processes discussed above and analyzed several possibilities for stabilization of TiO_x cluster formation in DC magnetron sputtering from a pure titanium target in a gas aggregation cluster source. Using oxygen, we investigated the role of reactive gas flow in the different processes and studied its role in stabilizing cluster formation. We show that the stability of cluster deposition under different conditions depends strongly on the amount of reactive gas and the dominant mechanism, and we report the specific optimal conditions which lead to highly stable cluster formation.

Experimental

The planar magnetron was installed in a self-constructed gas aggregation chamber (Peter et al. 2013). It equipped with a 2-inch round titanium target (99.99 % purity) with 6 mm thickness. For TiO_x cluster generation, argon and small amount of oxygen were used as

working gas and reactive gas, respectively. The aggregation chamber was connected to the main chamber (deposition chamber) via an orifice with 3 mm in diameter.

The pressure in the aggregation source was set between 50 and 200 Pa and measured by a MKS Baratron. A MKS mass flow controller (200.0 SCCM) and Apex mass flow controller (1.000 SCCM) were applied to control the argon and oxygen flow, respectively. The Argon flow rate was in the range of 25–110 SCCM, and the range of applied oxygen flow was between 0.010 and 0.140 SCCM. The magnetron was connected to a DC power supply (MDX 500, Advanced Energy). In the present work, the used power was in the range of 30–100 W. The D.R. in each step was monitored by quartz crystal microbalance (QCM), which was placed in the deposition chamber, 6 cm away from the orifice of aggregation source. Evolution of cluster deposition was monitored for 25–45 min to observe a distinct trend in the evolution.

A turbo molecular pump (TMP) (Pfeiffer TMU 261) supported by a scroll pump (SP) (Varian SH 110) was linked to the deposition chamber for pumping down to about 10^{-5} Pa as background pressure before each experiment.

For monitoring the signal of the oxygen molecules escaped from the aggregation chamber, a quadrupole mass spectrometer (QMS) (Balzers Prisma QMS-QME200) equipped by a channeltron/Faraday detector was used. It was located in a tube attached to the main chamber separated by a variable valve to allow differential pumping by a turbo pump (Pfeiffer HiPace80). During the experiments, the mass spectrometer was adjusted to monitor only the oxygen (32 amu) and the Argon (40 amu) concentrations.

The chamber of the mass spectrometer was pumped down by a turbo pump (Pfeiffer HiPace80) to 10^{-7} Pa base pressure. The mass spectrometer chamber also was connected to the deposition chamber by a tube and variable valve. For cluster size evaluation, samples were prepared at the position of the QCM on silicon substrates. These samples were then analyzed by a SEM (Zeiss-Supra 55VP). Figure 1 shows our setup schematically.

Results and discussion

The effect of oxygen as an impurity species on cluster formation and cluster deposition from the gas

aggregation cluster source was investigated at different pressures. In all experiments, initially the target surface was cleaned by pure argon discharge. Depending on the target history, the time of the cleaning process was different. Directly after cleaning, no cluster deposition was detected as observed before (Peter et al. 2012). Afterward, oxygen as a reactive gas was added to the argon working gas in the aggregation chamber, and the D.R. was measured with a QCM monitor placed in the main chamber.

The first experiment was performed at 50 Pa by injecting 25 SCCM argon into the aggregation chamber. The discharge was run at 50 W, and different

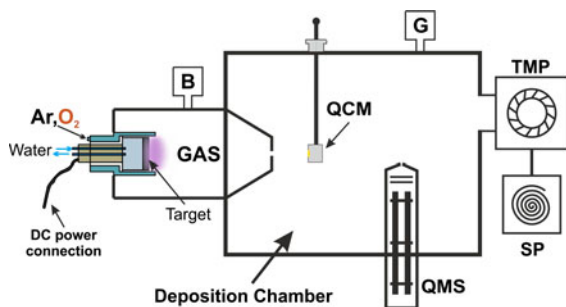


Fig. 1 Schematic of the experimental setup. A magnetron source is mounted in the GAS. A QCM and a QMS are used for recording cluster D.R. and the amount of oxygen molecules escaping from aggregation source, respectively. The system is evacuated by a TMP supported by a SP. A gauge (G) and a baratron (B) are used for measuring the pressure in the main chamber and aggregation chamber, respectively

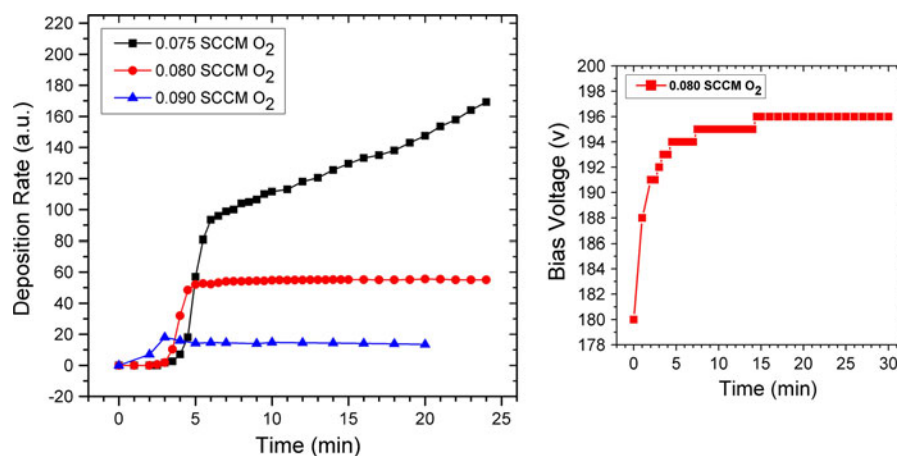


Fig. 2 Cluster D.R. evolution (*left*) at 50 Pa of argon pressure in the gas aggregation chamber and different oxygen flows. In all experiments, the magnetron power was 50 W. One notes that a change in oxygen flow strongly affects the D.R. curves. A

concentrations of oxygen were used. Some minutes after starting the oxygen flow, the D.R. increased dramatically and reached a knee as shown in Fig. 2. For 0.080 SCCM, the D.R. was highly stable after the initial increase.

Apparently at the beginning, after adding oxygen to the gas aggregation chamber, sticking to the chamber walls, and surface target poisoning are dominant processes for oxygen consumption, while the oxidation of sputtered atoms in the gas volume is of minor importance. Therefore, a delay in deposition is observed which depends on the applied oxygen flow. After this primarily step, metal atom oxidation is the main process in the gas volume. When the number of oxide molecules becomes high enough, the cluster nucleation process—and in the next step the growing process—is started. These processes will continue until equilibrium between sputtering rate and cluster formation is established and the knee is reached in the D.R. curve. Afterward changes in the local poisoning area on the target control the D.R. evolution.

If the oxygen flow is equal to the amount which is needed for stabilization, the poisoned region will remain constant. Under this condition, the sputtering rate is also constant, and cluster formation as well as the D.R. is stable. Here, the rate of enlarging the poisoned regions on the target by the poisoning processes discussed above and the rate of surface cleaning by impact of ions are in equilibrium. The evolution of bias voltage during cluster deposition

highly stable D.R. for long time is only achieved for one oxygen flow. The magnetron bias voltage evolution during deposition for this stable case is shown on *right*

(Fig. 2, left) also confirms that the fraction of poisoned regions on the target is stable. In other cases, where the oxygen flow is lower or higher than the optimum flow, the equilibrium between poisoning and cleaning on the target surface cannot be established completely, and variations in the poisoned area lead to a drift in the D.R. (Fig. 2).

We note that, when the cluster formation processes sets in, less amount of oxygen—in comparison with the initial steps—is available for poisoning because some oxygen is consumed for cluster production. Thus, at the oxygen flows lower than required for the stable case, the poisoned areas start to shrink because the cleaning process by impacting argon ions is stronger than target poisoning processes, and consequently, the target surface will be cleaned gently. Enlarging the cleaned area enhances the sputtering rate of metal atoms which leads to more cluster nucleation. Therefore, an increase in cluster generation is recorded (Fig. 2). We expect that, after a long time, a constant D.R. might even be established in this case.

In the opposite case, by increasing the oxygen flow rate above the optimum value, the rate of target poisoning gets higher than the rate of the cleaning process by incoming argon ions. Then, due to enlargement of the poisoned area, the sputtering rate and subsequently the cluster formation will diminish gradually.

We mention that beside cluster seeding by sputtered-off pure metal atoms, direct sputtering of oxide molecules (TiO_x) from the surface target can also contribute to the clustering processes. These TiO_x molecules can be produced on some clean parts of the target by binding of arriving oxygen atoms with surface titanium atoms if they will be sputtered off by impacting argon ions immediately after creation.

It is important to note that, at low pressure in the aggregation chamber (50 Pa), due to the long mean free path, the contribution of returning oxidized atoms in surface poisoning is expected to be weak because they have only a low probability to collide with other particles and return to surface. Thus, direct diffusion or flow of oxygen to the target is the dominant mechanisms for surface poisoning.

To study the role of the oxygen concentration in clustering and in poisoning of the surface in more details, a mass spectrometer was installed and linked to the main chamber in order to monitor the oxygen

molecules which escaped from the aggregation chamber.

For the stable case (0.080 SCCM), the O_2 signal does not change in the first 2–3 min (Fig. 3), indicating that in this period (as discussed above), the oxygen is consumed mainly by the available sputtered metal atoms on the aggregation chamber walls (which were produced during the cleaning process), and by the poisoning process on the target surface. After these preliminary processes, oxidation of sputtered metal atoms in the gas volume is dominant. Consequently, clustering processes are initiated, and then the residual oxygen molecules escape from the cluster source and the spectrometer signal increases. When a relative equilibrium among sputter rate, cluster formation, and surface poisoning is established after the knee region in Fig. 2, the oxygen signal increases very gently. This trend of the oxygen signal can be explained by saturation of the adsorption of oxygen molecules on the aggregation chamber walls. When the number of oxygen molecules arriving at the walls reaches to the saturation value, more oxygen molecules can escape from the aggregation chamber and increase the signal of oxygen molecules.

For other oxygen flows, the plateau of the oxygen signal emerges at different times (Fig. 3). It is clear that the oxygen signal is affected not only by the absolute value of oxygen flow, but also by the clustering and poisoning process under each condition. The plateau of the oxygen signal for 0.090 SCCM is nearly 2.5 times higher than the plateau for the

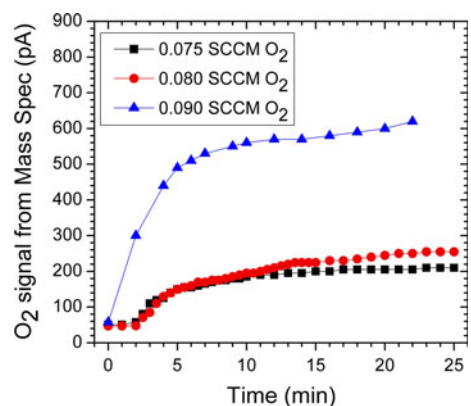


Fig. 3 Mass spectrometer signal evolutions for different oxygen flows at constant argon pressure (50 Pa). The amount of escaped oxygen particles strongly depends on the oxygen flow as well as the dominant poisoning mechanisms in each condition

stabilized case (0.080 SCCM of oxygen flow). The higher oxidation rates of the target and lower sputtering rate at 0.090 SCCM oxygen flow lead to an escape of a high amount of oxygen from the aggregation chamber after the initial stages. In contrast, in the case of 0.075 SCCM oxygen flow, the oxygen signal—after an initial increase—shows only a small difference in comparison with the signal for the stabilized case. The absolute amount of oxygen flow is the main factor for this difference. As we discussed before, at 0.075 SCCM, the consumption of oxygen for the poisoning process is lower than for the stable case, but at the same time, due to the higher sputtering rate, more oxygen is consumed in clustering. Therefore, the higher consumption rate of oxygen for clustering can compensate the lower rate which is used for poisoning, and thus the oxygen signal is mostly flat after the initial increase.

In a next step, we studied the effect of magnetron power on cluster deposition. As shown in Fig. 4, the stable part of the deposition curve strongly depends to the magnetron power.

Since the number of sputtered atoms strongly depends on the applied power, higher cluster nucleation rates can be achieved by increasing magnetron power. We noted that in the investigated range from 30 to 100 W, the oxygen flow required to obtain stable

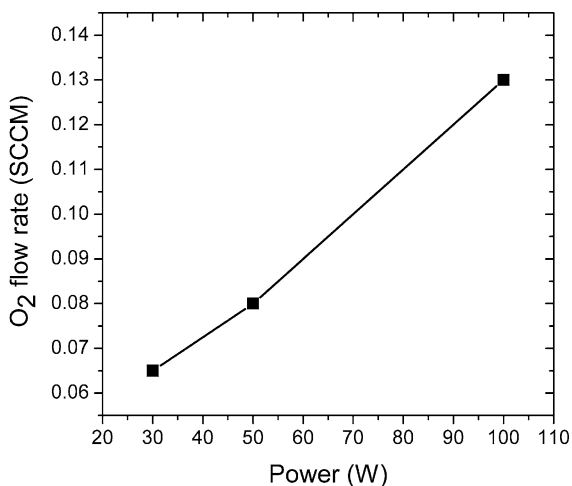


Fig. 4 Necessary oxygen flow for stabilization of cluster formation at different powers. The oxygen flow was changed for each feeding power to find the flow for stabilized cluster formation. One notes an almost linear relationship between power and optimum oxygen flow at constant argon pressure (50 Pa)

cluster deposition depends almost linearly on the magnetron power (Fig. 4).

Cases of stable operation are shown in Fig. 5a for 30 and 50 W applied power. Due to higher sputtering rate at higher power, the stable part is shifted to higher D.R.s.

The results obtained for the evolutions of the D.R. at 100 W (Fig. 5b) are mostly similar to the behavior at lower powers, but they also show some specific trends not seen in at lower power. A longer delay in cluster formation and a shift of the knee in the D.R. curve are the first difference. This delay was observed for all investigated oxygen concentrations. The other difference was observed for the specific oxygen flow of 0.130 SCCM. According to the results obtained in the experiments for lower powers, it was expected to achieve a highly stable cluster D.R. for 100 W power at an oxygen admixture around 0.130 SCCM. While at this conditions, the D.R. curve shows a first knee before the expected knee point, then remains stable as expected, but for just 8–10 min, and subsequently starts to increase again (Fig. 5b). It seems, that more investigations are required to clarify this behavior at high power. The drop of the D.R. at the higher oxygen flow of 0.140 SCCM at longer times is attributed to target poisoning.

At higher feeding power, the number of accessible Ti atoms in the aggregation chamber increases, which should lead to the formation of larger clusters. Similar studies on Ni (Hihara and Sumiyama 1998) and Ag (Polonskyi et al. 2012) also showed bigger clusters at higher magnetron power. To test the effect of magnetron power on the particle size distribution for Ti, we took SEM pictures of the deposited clusters prepared under stable conditions. One sees in Fig. 6 that the mean particles size is the same for different magnetron powers. However, the amount of deposited clusters increases with feeding power.

It seems that cluster growth is reduced at higher power in the present case. To find the reason for this unexpected observation, the temperature evolution of the aggregation chamber was monitored during deposition as temperature is known to affect particle size (Shyjumon et al. 2006). For both conditions of lower power (30 and 50 W), the temperature of the aggregation chamber walls (outside) was constant and its value remained at the initial temperature throughout of deposition process. In contrast, at the same time at 100 W, the temperature increased by 8–10 K. It is

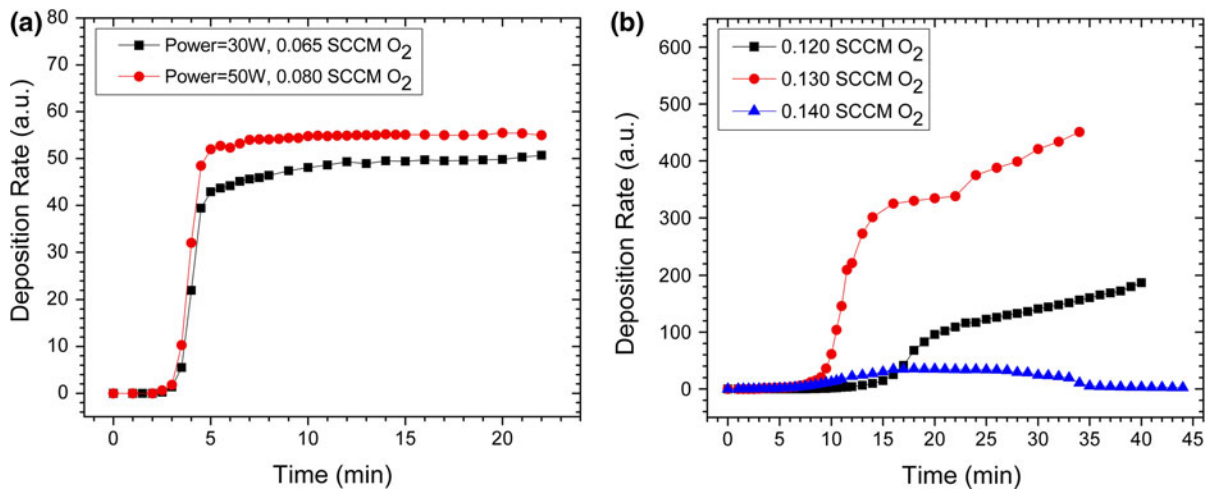


Fig. 5 **a** Examples of stable cluster deposition for operation at low magnetron powers. **b** Evolution of the D.R. for different oxygen concentrations at 100 W. Here stable deposition is not

clear that the temperature increase of the inner chamber walls was considerably higher than measured from outside of chamber. Processes such as transfer of thermal energy from the magnetron to the gas volume by argon and sputtered atoms (Kashtanov et al. 2010), oxidation and clustering processes in the gas volume, and also recombination of charged particles are noticeable factors for elevating the temperature in the gas aggregation cluster source. Although, the role of the individual mechanisms is not well-known yet, and further investigations are needed to clarify this subject, the increase in the temperature of the inner chamber walls can well explain the absence of cluster growth at higher magnetron power.

To determine whether a stabilization of the deposition process is also possible at other argon pressures, we analyzed the deposition at different pressures and with different oxygen concentrations. At 100 Pa, corresponding to 51 SCCM argon flux into the gas aggregation source (GAS), the trend of the initial stage for evolution of the D.R. was identical to that at 50 Pa, but when the deposition curve reached to the knee, the D.R. started to drop and after some minutes reached zero (Fig. 7a).

By varying in oxygen flow we did not reach to a long-term stabilization of the D.R. Changing the oxygen amount only leads to a change in the time of the appearance of the peak and in the width of the maximum, but not to stable deposition. Higher oxygen flows lead to earlier peaks due to faster oxidation of

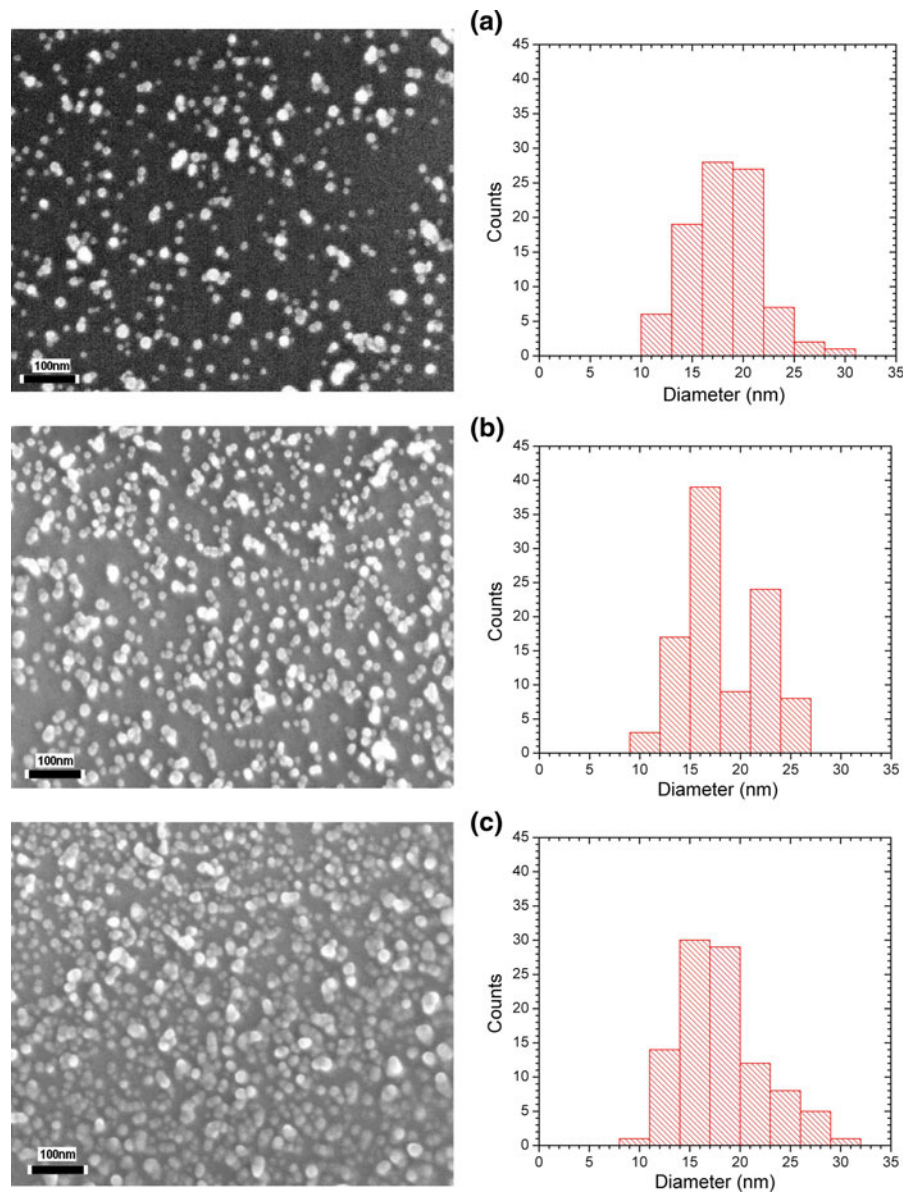
observed within the experimental observation time. All experiments were carried out at 50 Pa of argon, and the oxygen flow was varied to obtain stable deposition

available sputtered atoms in the volume and also faster oxidation of the target surface. The highest full width at half maximum (FWHM) of the deposition at 100 Pa was obtained for 0.040 SCCM oxygen flow. At oxygen concentrations above or below this value, the FWHM was reduced (about 35 % for both cases), indicating that further changes in oxygen flow will not result in stable deposition (Fig. 7a).

The observation that stable deposition cannot be achieved at 100 Pa pressure in the above oxygen concentration range can be explained by the fact that the number of metal-oxide molecules returning to the target under this condition is quite high. The returning oxidized atoms expand the poisoned region and decrease the sputtering rate quickly and impacting argon ions are not able to provide a large clean area on the target. Thus, the sputter rate will not be sufficient for cluster nucleation. The evolution of bias voltage (Fig. 7a) shows a continuous growth which is due to the continuous enlargement of the poisoned regions on the target.

The oxygen signal evolutions in the mass spectrometer for different concentrations of oxygen is in agreement with this notion (Fig. 7b). After an initial period, where all oxygen particles are consumed for target poisoning, sticking to chamber walls, and clustering, the signals grows continuously. The increasing poisoned region on the target and the drop of cluster formation leads to an escape the most of the free oxygen molecules from the aggregation chamber,

Fig. 6 SEM images (*left*) and corresponding histograms (*right*) of the samples prepared under conditions of stable D.R. with different powers and constant argon pressure (50 Pa). **a** Power = 30 W and O₂ flow = 0.065 SCCM **b** Power = 50 W and O₂ flow = 0.080 SCCM **c** Power = 100 W and O₂ flow = 0.130 SCCM. In all cases, the mean particle size is around 18 nm



and hence to an increasing oxygen signal in the mass spectrometer.

Finally, we studied the clustering process and the effect of oxygen at 200 Pa by applying 107 SCCM argon flow to the GAS. At this pressure the D.R. shows a maximum similar as at 100 Pa. However, at 200 Pa, the D.R. does not fall to zero, but to a constant, stable value (Fig. 8a), while the oxygen signal evolutions for different oxygen flows are similar to the behavior at 100 Pa. This indicates that the underlying processes at both pressures are almost the same. As seen in Fig. 8a, the stable part for

different oxygen flows has the same absolute amount. A possible explanation for this behavior could be the high number of argon ions impacting on the target at 200 Pa. These ions can apparently sputter off enough TiO_x molecules from the target surface to enable cluster formation in the gas volume. At constant power and constant pressure, the impingement rate of argon ions on the target surface is almost constant, therefore, cluster seeding is similar for the different applied oxygen concentrations.

As for an argon pressure of 100 Pa, the peak in the D.R. curve shifts to later times with decreasing oxygen

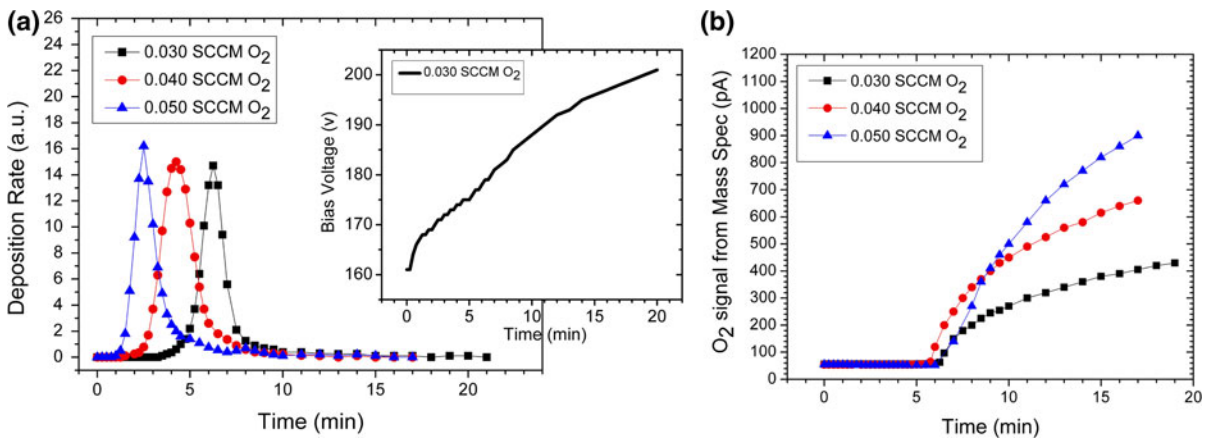


Fig. 7 **a** Cluster D.R. and bias voltage evolution for different oxygen flows during deposition at a higher argon pressure of 100 Pa. **b** Evolution of the mass spectrometer signal for escaped oxygen molecules (mass = 32 amu) from the aggregation

chamber during cluster deposition. Measurements were done at a constant power of 50 W. Different oxygen flows only change the time of the peak appearance and the width of the peak, but a non-zero stable deposition is not reached

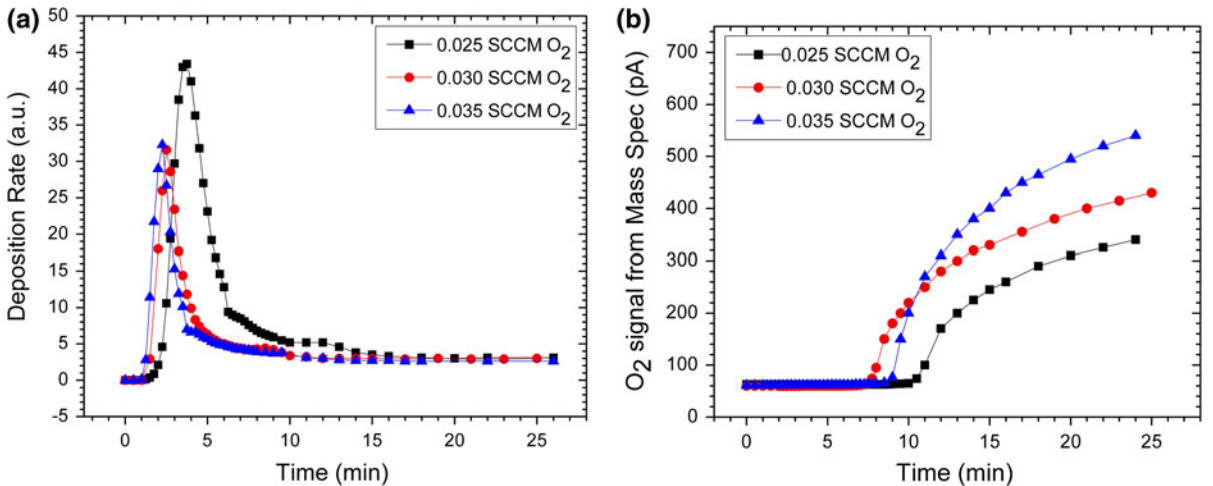


Fig. 8 **a** Evolution of the cluster D.R. at 200 Pa argon pressure. An identical stable non-zero plateau is reached after a maximum for all oxygen flows. **b** Evolution of the mass spectrometer

signal for the oxygen molecules (mass = 32 amu) escaped from the aggregation chamber during cluster deposition

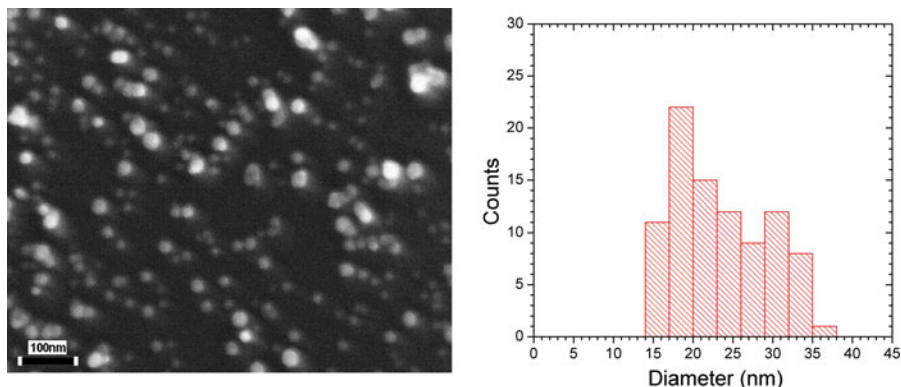
flow (Fig. 8a). Additionally, at this pressure the cluster deposition for the lowest oxygen flow (0.025 SCCM) shows a higher peak and also a higher total amount of deposited material than for other oxygen flows (Fig. 8a). It seems that the lower amount of oxygen arriving at the target surface provides a larger clean area on the target surface during the initial stage. Thus, a higher sputtering rate provides higher cluster seeding in this regime. For the same reason, the oxidation of sputtered atoms in the gas volume is initially decreased. Consequently, the starting time of cluster deposition, the appearance of the peak, and also the

time for reaching the stable part are delayed. At oxygen flows lower than 0.025 SCCM, no cluster deposition was recorded by QCM.

Due to different oxygen consumption in the aggregation chamber for different oxygen flows, the onset of the oxygen signal for 200 Pa (Fig. 8b) depends on the absolute oxygen amount.

The size distribution of the clusters formed in the stable part at 200 Pa and its related histogram is shown in Fig. 9. At high pressure, the small mean free path and the resulting high collision frequency leads to the formation of large clusters.

Fig. 9 SEM image (*left*) and corresponding histogram (*right*) of a sample prepared in the stable part of D.R. curve at 200 Pa. The oxygen flow rate was 0.030 SCCM, and the magnetron power was 50 W. The mean clusters size is about 23 nm



Conclusions

Using Ti and oxygen as examples, we studied the influence of reactive gas admixtures on the formation of TiO_x clusters during reactive DC magnetron sputtering in a gas aggregation chamber and explored regimes of stable cluster formation. We could stabilize TiO_x cluster formation by adjusting the oxygen flow at an argon pressure of 50 Pa. The range of oxygen flow for stable operation is very narrow and depends strongly on the magnetron power. At an argon pressure of 200 Pa, stable cluster formation is obtained after going through a maximum. The stable rate turned out to be independent of the oxygen flow in the investigated range. At 100 Pa, the D.R. also goes through a maximum, but subsequently drops down to zero. The crucial role of oxygen is also confirmed by mass spectrometry. The results are explained by a competition between oxygen induced cluster nucleation and target poisoning.

Acknowledgments This work was supported by the German Research Foundation (DFG) within the framework of the Collaborative Research Center SFB TR 24, subproject B13. One of us (A. M. Ahadi) is grateful to the Iran Ministry of Science for financial support. We would also like to thank Stefan Rehders for the technical construction of the cluster source, Rainer Kloth for technical support, and C. Schütte for her comments.

References

- Anders C, Bringa EM, Ziegenhain G, Urbassek HM (2011) Stopping of hypervelocity clusters in solids. *New J Phys* 13:113019. doi:10.1088/1367-2630/13/11/113019
- Baletto F, Ferrando R (2005) Structural properties of nanoclusters: energetic, thermodynamic, and kinetic effects. *Rev Mod Phys* 77:371–423. doi:10.1103/RevModPhys.77.371
- Bauer G, Pittner F, Schalkhammer T (1999) Metal nano-cluster biosensors. *Microchim Acta* 114:107–114. doi:10.1007/PL00021395
- Biederman H (2011) Nanocomposites and nanostructures based on plasma polymers. *Surf Coat Technol* 205:S10–S14. doi:10.1016/j.surfcoat.2011.03.115
- De Heer W (1993) The physics of simple metal clusters: experimental aspects and simple models. *Rev Mod Phys* 65:611–676. doi:10.1103/RevModPhys.65.611
- Depla D, Mahieu S (2008) Reactive sputter deposition, chap 5. Springer, Berlin/Heidelberg
- Drabik M, Choukourou A, Artemenko A et al (2011a) Structure and composition of titanium nanocluster films prepared by a gas aggregation cluster source. *J Phys Chem C* 115:20937–20944. doi:10.1021/jp2059485
- Drabik M, Choukourou A, Artemenko A et al (2011b) Morphology of titanium nanocluster films prepared by gas aggregation cluster source. *Plasma Process Polym* 8:640–650. doi:10.1002/ppap.201000126
- Faupel F, Zaporozhtchenko V, Strunskus T, Elbahri M (2010) Metal-polymer nanocomposites for functional applications. *Adv Eng Mater* 12:1177–1190. doi:10.1002/adem.201090036
- Grabowska E, Remita H, Zaleska A (2010) Photocatalytic activity of TiO_2 immobilized on glass beads. *Physicochem Probl Miner Process* 45:29–38
- Haberland H, Karrais M, Mall M, Thurner Y (1992) Thin films from energetic cluster impact: a feasibility study. *J Vac Sci Technol A* 10:3266–3271. doi:10.1116/1.577853
- Hihara T, Sumiyama K (1998) Formation and size control of a Ni cluster by plasma gas condensation. *J Appl Phys* 84:5270. doi:10.1063/1.368776
- Kashtanov PV, Smirnov BM, Hippler R (2007) Magnetron plasma and nanotechnology. *Phys Usp* 50:455. doi:10.1070/PU2007v050n05ABEH006138
- Kashtanov PV, Smirnov BM, Hippler R (2010) Efficiency of cluster generation in a magnetron discharge. *EPL (Europhys Lett)* 91:63001. doi:10.1209/0295-5075/91/63001
- Kortshagen U (2009) Nonthermal plasma synthesis of semiconductor nanocrystals. *J Phys D Appl Phys* 42:113001. doi:10.1088/0022-3727/42/11/113001
- Marek A, Valter J, Kadlec S, Vyskočil J (2011) Gas aggregation nanocluster source—reactive sputter deposition of copper and titanium nanoclusters. *Surf Coat Technol* 205:S573–S576. doi:10.1016/j.surfcoat.2010.12.027

- Palmer RE, Pratontep S, Boyen H-G (2003) Nanostructured surfaces from size-selected clusters. *Nat Mater* 2:443–448. doi:[10.1038/nmat897](https://doi.org/10.1038/nmat897)
- Peter T, Polonskyi O, Gojdka B et al (2012) Influence of reactive gas admixture on transition metal cluster nucleation in a gas aggregation cluster source. *J Appl Phys* 112:114321. doi:[10.1063/1.4768528](https://doi.org/10.1063/1.4768528)
- Peter T, Rehders S, Schürmann U et al (2013) High rate deposition system for metal-cluster/SiO_xC_yH_z-polymer nanocomposite thin films. *J Nanoparticle Res* 15:1710. doi:[10.1007/s11051-013-1710-6](https://doi.org/10.1007/s11051-013-1710-6)
- Polonskyi O, Solar P, Kylian O et al (2012) Nanocomposite metal/plasma polymer films prepared by means of gas aggregation cluster source. *Thin Solid Films* 520:4155–4162. doi:[10.1016/j.tsf.2011.04.100](https://doi.org/10.1016/j.tsf.2011.04.100)
- Safi I (2000) Recent aspects concerning DC reactive magnetron sputtering of thin films: a review. *Surf Coat Technol* 127:203–218. doi:[10.1016/S0257-8972\(00\)00566-1](https://doi.org/10.1016/S0257-8972(00)00566-1)
- Schultes G, Schmidt M, Truar M et al (2007) Co-deposition of silver nanoclusters and sputtered alumina for sensor devices. *Thin Solid Films* 515:7790–7797. doi:[10.1016/j.tsf.2007.03.183](https://doi.org/10.1016/j.tsf.2007.03.183)
- Shyjumon I, Gopinadhan M, Helm CA et al (2006) Deposition of titanium/titanium oxide clusters produced by magnetron sputtering. *Thin Solid Films* 500:41–51. doi:[10.1016/j.tsf.2005.11.006](https://doi.org/10.1016/j.tsf.2005.11.006)
- Smirnov BM (2000) Cluster plasma. *Phys Usp* 43:453–491. doi:[10.1070/PU2000v043n05ABEH000722](https://doi.org/10.1070/PU2000v043n05ABEH000722)
- Smirnov BM (2003) Generation of cluster beams. *Phys Usp* 46:589–628. doi:[10.1070/PU2003v046n06ABEH001381](https://doi.org/10.1070/PU2003v046n06ABEH001381)
- Wegner K, Piseri P, Tafreshi HV, Milani P (2006) Cluster beam deposition: a tool for nanoscale science and technology. *J Phys D Appl Phys* 39:R439–R459. doi:[10.1088/0022-3727/39/22/R02](https://doi.org/10.1088/0022-3727/39/22/R02)
- Wilcoxon JP, Abrams BL (2006) Synthesis, structure and properties of metal nanoclusters. *Chem Soc Rev* 35:1162–1194. doi:[10.1039/b517312b](https://doi.org/10.1039/b517312b)